diversity

MDPI

Article

Systematic of a Massively Constructed Specimen of *Iguanodon galvensis* (Ornithopoda, Iguanodontidae) from the Early Barremian (Early Cretaceous) of Eastern Spain

Josué García-Cobeña *, Francisco J. Verdú and Alberto Cobos

Fundación Conjunto Paleontológico de Teruel-Dinópolis/Museo Aragonés de Paleontología, Av. Sagunto S/N, 44002 Teruel, Spain; verdu@fundaciondinopolis.org (F.J.V.); cobos@dinopolis.com (A.C.)
* Correspondence: gcobena@fundaciondinopolis.org

Abstract: Styracosternan ornithopods are plenty abundant in the Lower Cretaceous fossil record of Europe. In particular, *Iguanodon*, the second genus of dinosaurs described worldwide, has been found in UK, Belgium, France, Germany, and Spain, evidencing a wide geographical distribution. Currently, the genus *Iguanodon* comprises two species, the type species *I. bernissartensis* from the late Barremian–Aptian of Europe and *I. galvensis* from the early Barremian of Teruel, Spain. The latter species is well known mainly from perinate and juvenile specimens. Here, axial and appendicular fossils of an adult, large and massively constructed ornithopod from the lower Barremian (Lower Cretaceous) Camarillas Formation of Galve (province of Teruel, Spain) are described. Fossil dimensions and some osteological evidence reveal that the specimen was a large (roughly 10 m long) ornithopod. An autapomorphic feature in the ischium and other characters allow us to ascribe this specimen to *I. galvensis*. In addition, postcranial co-ossification and fusion of the neurocentral suture indicate that the specimen was skeletally mature. Part of the material studied here was unknown in adults of *I. galvensis*, providing a better knowledge of the axial and appendicular region of this species.

Keywords: styracosterna; *Iguanodon*; systematics; comparative anatomy; Lower Cretaceous; Teruel

Citation: García-Cobeña, J.; Verdú, F.J.; Cobos, A. Systematic of a Massively Constructed Specimen of *Iguanodon galvensis* (Ornithopoda, Iguanodontidae) from the Early Barremian (Early Cretaceous) of Eastern Spain. *Diversity* **2024**, *16*, 586. https://doi.org/10.3390/d16090586

Received: 12 July 2024
Revised: 9 September 2024
Accepted: 12 September 2024
Published: 17 September 2024

1. Introduction

Ornithopods are the most common dinosaurs registered in the Lower Cretaceous sediments of Europe. This group is represented by small hypsilophodontids, such as *Hypsilophodon foxii* (e.g., [1,2]), *Gideonmantellia* [3], and *Vectidromeus* [4]; scarce rhabdodontomorphans [5]; small dryosaurids like *Valdosaurus* [6]; and medium to large styracosternans (e.g., [7–23]). The latter is the most prominent and well-known group in Europe, especially in the pre-Albian sediments, with an exquisite representation constituted by the medium-sized *Mantellisaurus* [8,24], *Morelladon* [16], *Brighstoneus* [22], and *Portellsaurus* [23] and the large-sized taxa *Magnamanus* [25], *Iguanodon galvensis* [18,26], and *I. bernissartensis* [7,15,17]. In the Iberian Peninsula, styracosternans are abundant in the Barremian deposits of the Lusitanian Basin [27–29], the Cameros Basin [25,30], the Cuenca Basin [14,31], and the Maestrazgo Basin [15–18,20,21,23–35].

A remarkable sample of specimens from embryos to adults of the large and robust *I. galvensis* has been described in the lower Barremian Camarillas Formation of Spain [18,21,26]. Albeit this species is represented by all the ontogenetic stages, "fully" grown specimens are less known. In fact, the holotype is a partial sub-adult skeleton that reached 7 m in length [26]. The largest specimen referred to *I. galvensis* (10 m long) collected to date is only represented by a set of cervical and dorsal vertebrae and dorsal ribs [21], which have yielded new data on the discrimination of both species of *Iguanodon* due to the anatomical variability of the dorsal vertebrae within the dorsal region.

Hence, cranial, axial, and appendicular fossils of a large specimen of *I. galvensis* from the lower Barremian Camarillas Formation in the municipality of Galve (province of Teruel,

eastern Spain) are reported. The main aims of this work are to (1) provide a detailed description of these fossils; (2) test dorsal vertebrae into a multivariate component analysis to determinate morphotype affinities; (3) compare the fossil sample with those of other styracosternans from the Lower Cretaceous of Europe; and (4) determine and discuss the taxonomic status of the specimen, justifying the assignation to this species. This specimen increases our knowledge on the anatomy of large specimens of *I. galvensis*, providing bones scarcely known.

1.1. Institutional Abbreviations

FCPTD, Fundación Conjunto Paleontológico de Teruel-Dinópolis, Teruel, Spain; GPIT, Institut und Museum für Geologie und Paläontologie of the Universität Tübingen, Tübingen, Germany; MIWG, Museum of Isle of Wight Geology, Dinosaur Isle Museum, Isle of Wigth, UK; MAP, Museo Aragonés de Paleontología (FCPTD), Teruel, Spain. MNS, Museo Numantino de Soria, Soria, Spain; NHMUK, The Natural History Museum of Natural Sciences, London, UK; RBINS, Royal Belgium Institute of Natural Sciences, Brussels, Belgium.

1.2. Other Abbreviations

CM, Cabra de Mora site, Cabra de Mora, Spain; CMP, Mas de la Parreta Carry-Mas de Sabater site, Morella, Spain; CT, El Castellar sites, El Castellar, Spain; DS, Las Dehesillas site, Aliaga, Spain; SC, San Cristóbal site, Galve, Spain.

2. Geographical and Geological Settings

The municipality of Galve is located 60 km north of Teruel, in the province of Teruel (Aragón, north-eastern Spain; Figure 1A,B). SC-4 site was found within the PAMESA Cerámica Compacto S.L.U. (previously SILBECO Minerales Cerámicos S.A.) clay mine during the paleontological tasks carried out by the FCPTD in the area. It is 500 m south of this municipality and lies in the Maestrazgo Global Geopark (Aragonian Branch, Iberian Range).

Geologically, the SC-4 site is placed on the Galve sub-basin, in the western Maestrazgo Basin, Iberian Basin [36] (Figure 1C,D). This geological area is mainly constituted by continental and marine deposits from the Kimmeridgian to the early Aptian [37,38] (Figure 1E). Concretely, the SC-4 site lies in facies of the Camarillas Formation. This lithostratigraphic unit was defined by [39] and later redefined by [40]. Stratigraphically, the Camarillas Formation is composed of white and grey sandstones and conglomerates, red and varicolored mudstones and some layers of marlstones and limestones [37,41] (Figure 1F). Originally, this unit was interpreted as a fluvial system with low sinuosity paleochannels [37,40,42]. Moreover, the depositional system of the Camarillas Formation is interpreted as a back barrier system with lagoonal environments in the Galve sub-basin [43]. Recently, this was considered as a tide-dominated estuary which evolved into a barrier island–tidal inlet in the same sub-basin [41].

The base of the Camarillas Formation overlies the lacustrine–palustrine deposits of the El Castellar Formation, aged as late Hauterivian–early Barremian [44], with a neat contact [39,40], while the upper limit changes gradually upwards to the shallow carbonate platform deposits of the Artoles Formation [37,42], dated as early to late Barremian [45].

The Camarillas Formation was established as early Barremian on the basis on charophytes [44], spores and pollen [46], and ostracods [47].

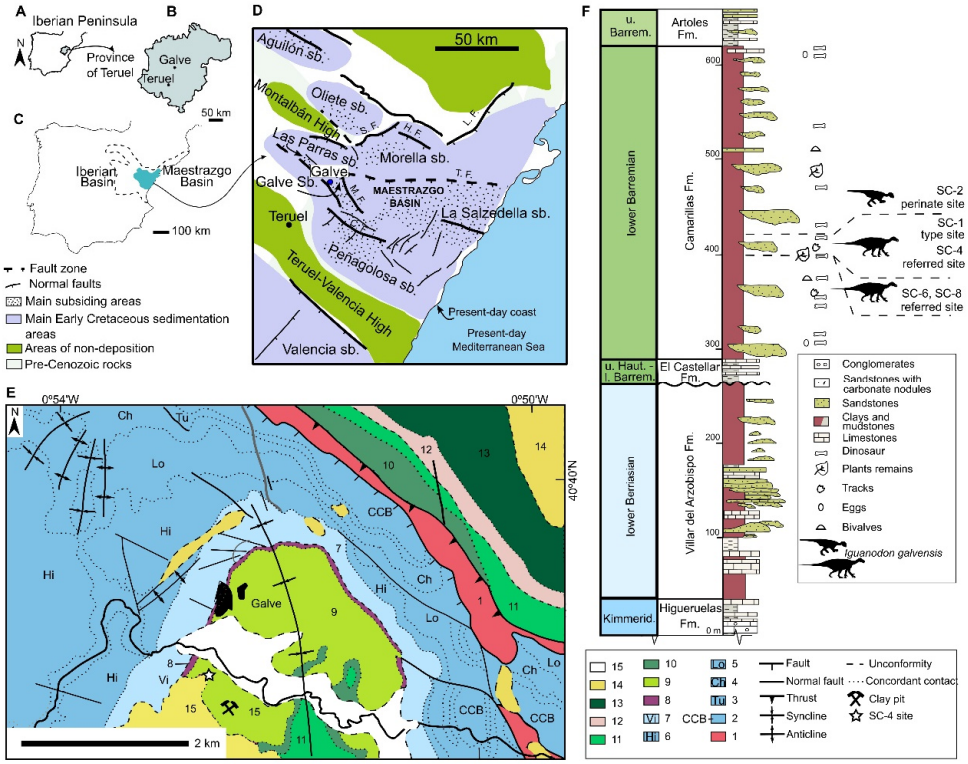

Figure 1. Geographical location of the SC-4 site in the municipality of Galve, Teruel, Spain (**A**,**B**). Geological situation of the SC-4 site at the Maestrazgo Basin, eastern Iberian Basin, redrawn from [48] (**C**,**D**). Geological map of the municipality of Galve, redrawn and modified from [48] (**E**). Stratigraphic section in the surroundings of Galve, redrawn and modified from [37,49]; ages are in accordance with [50] (**F**). Abbreviations: 1, Upper Triassic (Keuper); 2, Cortes de Tajuña, Cuevas Labradas and Barahona Formations (CCB); 3, Turmiel Formation (Tu); 4, Chelva Formation (Ch); 5, Loriguilla Formation (Lo); 6, Higueruelas Formation (Hi); 7, Villar del Arzobispo Formation (Vi); 8, El Castellar Formation; 9, Camarillas Formation; 10, Artoles Formation; 11, Morella Formation; 12, Utrillas Formation; 13, Upper Cretaceous; 14, Cenozoic; and 15, Quaternary. Abbreviations: Barrem., Barremian; Haut., Hauterivian; Kimmerid., Kimmeridgian; l, lower; u., upper.

2.1. Comments

The material found at the SC-4 site was in a lateral change of facies, between red and grey shales. Consequently, some fossils from the same site display changes in coloration. In addition, most of the remains show an oblique distortion with respect to the longitudinal axis.

2.2. Faunal and Flora Background

Fossils of styracosternan-like ornithopods are the most common in the Camarillas Formation (e.g., [18,19,21,26,33,35,51–56]). Nevertheless, there also is a record of small, basal ornithopods [3] and dryosaurids [57,58]. Theropods are represented by fossils of spinosaurids, non-avian ceolurosaurians, and allosauroids [58–63]. Sauropods are constituted by titanosauriforms [58]. In addition, there are also fossils of other vertebrates such as chondrichthyans, such as hybodontid sharks [64,65], and osteichthyes, such as Lepidotes and teleosteans [58,64,65]; lissamphibians [58,64,65]; testudines [66,67]; crocodylomorphs [68,69]; pterosaurs [58]; squamata reptiles [58,64,65]; and mammals (e.g., [70,71]). Invertebrates such as ostracods and bivalves have also been studied [47,72].

Regarding flora and the palynological record, the Camarillas Formation has yielded not only macroremains, such as those of the chirolepidiacean *Pseudofrenelopsis*, but also schizaeacean spores and pollen of gymnosperms and angiosperms [46].

3. Materials and Methods

The SC-4 site was initially excavated in 2013 during the paleontological control of the Cerro de San Cristóbal site within the PAMESA clay mine. The tasks in the mine uncovered new remains, so this locality was excavated again in the campaigns of 2018, 2020, and 2021. The results of the excavations provided a huge number of osteological fossils that correspond to a single, large specimen of ornithopod, apart from paleobotanical remains [46]. All the material from the SC-4 site is housed at the MAP.

Fossils from this site are referred to a single individual based on their close distribution in the site, the consistent size and shape of the elements, and the absence of repetition among them. The fossils recovered are cranial, axial, and appendicular elements. Here, only the most complete and well-preserved fossils are described (Figure 2; Supplementary Data, File S1).

Figure 2. Fossils of SC-4 specimen over a silhouette of *I. bernissartensis*. Silhouette obtained from [73] for *I. bernissartensis*.

All the fossils were measured using a measuring tape or a digital caliper. The measurements are available in Supplementary Data, File S1. The material was described and compared with that of other large ornithopods from the Early Cretaceous of Europe in order to test the anatomical affinities and conduct a systematic study through comparative anatomy. The comparative study is based on first-hand examination of the material of *Iguanodon galvensis* (SC-4 specimen and other individuals), "*Delapparentia*", and *Proa* (AR-1/103) in the MAP collection. Furthermore, anatomical data of other large styracosternan ornithopods (e.g., *Barilium*, *Hypselospinus*, *Morelladon*, *I. bernissartensis*, *Mantellisaurus*, and *Proa*) were obtained from the available scientific literature. SC-4 ornithopod is not compared with *Portellsaurus* due to the lack of overlapping elements [23].

Furthermore, a multivariate principal component analysis (PCA) was carried out on a vertebral data set modified from [20,34]. It includes our own linear measurements of SC-4 specimen and data of other ornithopods obtained from other publications (Supplementary Data, Files S1 and S2). Data were analyzed using PAST v.3.0 software [74]. Deformed fossils have not been considered for these analyses. Only dorsal vertebrae are tested because both cervical and caudal analysis resulted in noisy scatter plots, which failed to discriminate different morphotypes [20,34].

Hereinafter, genus name is indicated only when it is monospecific, whereas a multispecific genus is abbreviated after the full mention of their genus name.

4. Systematic Paleontology

ORNITHOPODA Marsh, 1881 [75] sensu Madzia, Arbour, Boyd, Farke, Cruzado-Caballero, and Evans, 2021 [76].

IGUANODONTIA Dollo, 1888 [77] sensu Madzia, Arbour, Boyd, Farke, Cruzado-Caballero, and Evans, 2021 [76].

DRYOMORPHA Sereno, 1986 [78] sensu Madzia, Arbour, Boyd, Farke, Cruzado-Caballero, and Evans, 2021 [76].

ANKYLOPOLLEXIA Sereno, 1986 [78] sensu Sánchez-Fenollosa, Verdú, and Cobos 2023 [79].

STYRACOSTERNA Sereno, 1986 [78].

HADROSAURIFORMES Sereno, 1997 [80] sensu Sereno, 1998 [81].

IGUANODONTIDAE Sereno, 1998 [81] sensu Madzia, Arbour, Boyd, Farke, Cruzado-Caballero, and Evans, 2021 [76].

IGUANODON Mantell, 1825 [82].

IGUANODON GALVENSIS Verdú, Royo-Torres, Cobos, and Alcalá, 2015 [18].

Holotype. MAP-4787, a sub-adult specimen represented by disarticulated cranial and postcranial bones, these latter including elements of the axial skeleton and hindlimbs. In addition, some material was later included as part of the holotype: a neural arch (MAP-4789) and an ungual phalanx of a manus digit I (MAP-4790) [21].

Paratype and referred material. Specimens from all the ontogenetic series found at several bone sites [21,26,34].

Remarks. The revised diagnosis of *I. galvensis* is taken from that of [21], which was modified from [26].

IGUANODON GALVENSIS.

4.1. Material

A maxillary tooth (MAP-8523), four almost complete cervical vertebrae (MAP-8494, MAP-8501, MAP-8518, and MAP-8519) plus two partial neural arches (MAP-8511 and MAP-8513), two anterior dorsal vertebrae (MAP-8495 and MAP-8499), an almost complete caudal vertebra (MAP-8500), and a centrum of a middle caudal vertebra (MAP-4676) plus four fragmented centra (MAP-6899, MAP-6970, MAP-6972, and MAP-8510), seven cervical ribs (MAP-6889 and MAP-6893, MAP-8502, MAP-8503, MAP-8507, MAP-8514, MAP-8518, and MAP-8519), two dorsal ribs (MAP-8496 and MAP-8497), a complete chevron (MAP-8516), several ossified tendons (MAP-8522), a partial left (?) scapula (MAP-8517), a fragmented sternal (MAP-8520), a fragmented right ulna (MAP-8515), an almost complete right ischium (MAP-8498), a fragment of an ilium (?) (MAP-8505), a proximal fragment of a left tibia (MAP-8521), and an the epiphysis of a tibia (?) (MAP-8504) (Supplementary Data, File S1).

4.2. Description

Dentition: MAP-8523 is a worn, right maxillary crown (Figure 3; Supplementary Data, File S1). The labial surface is enamelled. This exhibits a distally placed, primary ridge and four accessory ridges: three mesial and one distal to the primary ridge (Figure 3A). There is not a cingulum. A groove for an adjacent tooth is present in distal view (Figure 3B).

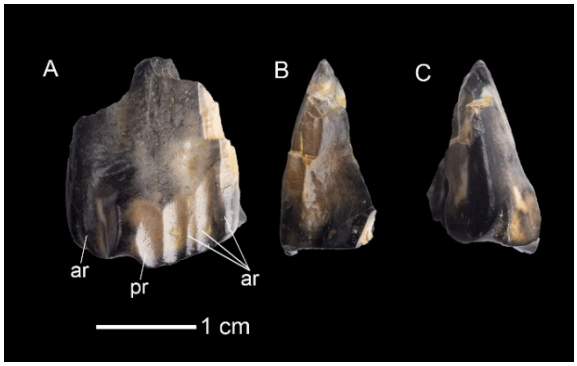

Figure 3. Right maxillary crown MAP-8523 of the *I. galvensis* specimen from the SC-4 site (Galve, Teruel, Spain). Views: labial (**A**), distal (**B**), and mesial (**C**). Abbreviations: ar, accessory ridges; pr, primary ridges.

Cervical vertebrae: The cervical region is represented by four complete vertebrae: MAP-8494, MAP-8501, MAP-8518, and MAP-8519 (Figure 4; Supplementary Data, File S1). They have a certain degree of dorsoventral distortion. All centra are opisthocoelous (e.g., Figure 4A,S) and longer than wide and high (e.g., Figure 4C,I; Supplementary Data, File S1). The anterior and posterior articular facets are wider than high and sub-elliptical to heart-shaped (e.g., Figure 4A,H,S). The lateral surfaces are craniocaudally concave and dorsoventrally convex. The ventral surface displays a longitudinal keel, which widens in more posterior centra, such as in MAP-8494 (Figure 4X). The parapophyses are robust, tubular, and have an elliptical cross-section. They are in the anteromedian region of the lateral surfaces (e.g., Figure 4I,O).

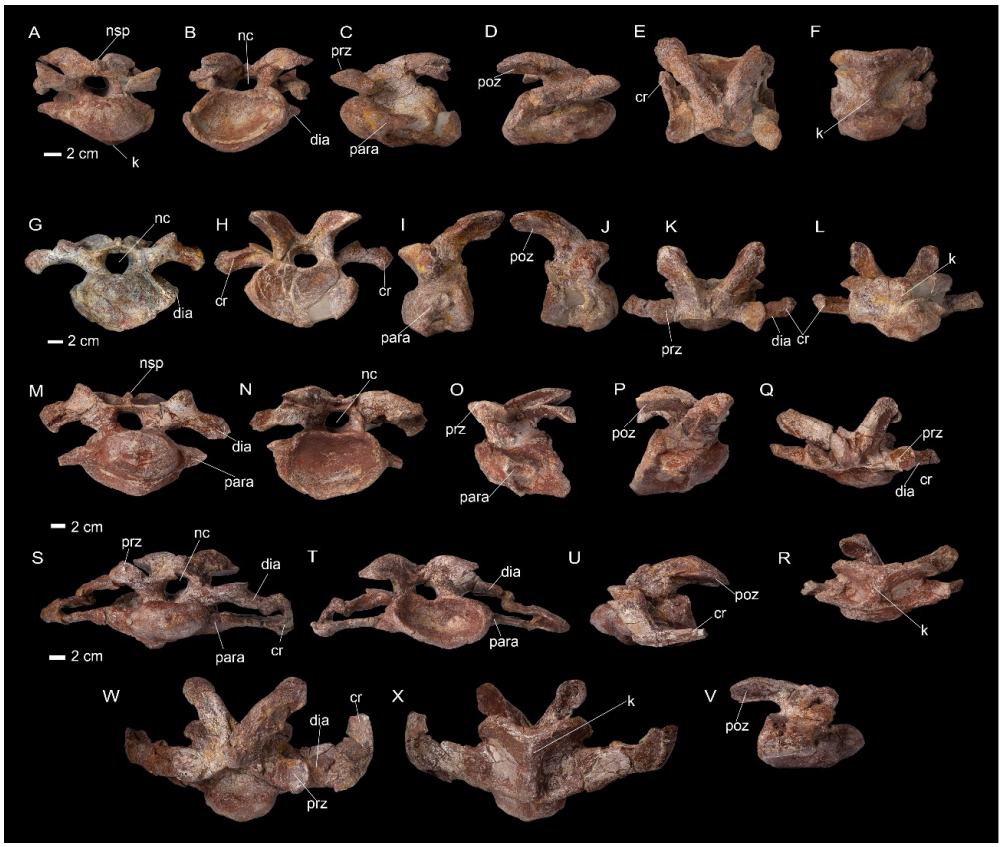

Figure 4. Cervical vertebrae of the *I. galvensis* specimen from the SC-4 site (Galve, Teruel, Spain). (**A**–**F**), MAP-8518. (**G**–**L**), MAP-8519. (**M**–**R**), MAP-8501. (**S**–**X**), MAP-8494. Views: cranial (**A**,**G**,**M**,**S**), caudal (**B**,**H**,**N**,**T**), left lateral (**C**,**I**,**O**,**U**), right lateral (**D**,**J**,**P**,**V**), dorsal (**E**,**K**,**Q**,**W**), and ventral (**F**,**L**,**R**,**X**). Abbreviations: cr, cervical rib; dia, diapophysis; k, keel; nsp, neural spine; para, parapophysis; poz, postzygapophysis; prz, prezygapophysis.

The neural arches are short in appearance but become longer towards most posterior vertebrae. The neurocentral sutures are sigmoid and closed (e.g., Figure 4B,G). The neural canal is subcircular and higher than wide in all the examples. The neural spines are thin, dorsally low laminae, which extend craniocaudally. The prezygapophyses are flat and elliptical (longer than wide). They are medially inclined and protrude cranially (more than the most anterior part of the centrum). The postzygapophyses are also flat and elliptical (longer than wide) and ventrolaterally directed (e.g., Figure 4J,P,V). The diapophyses are robust and subcircular in cross-section (e.g., Figure 4B,M). MAP-8518, MAP-8501, and MAP-8519 have parts of the cervical ribs sutured with either the parapophyses or diapophyses (Figure 4E,L,Q). In contrast, MAP-8494 has complete ribs fully fused with both the parapophyses and diapophyses (Figure 4U). In addition, there are two isolated and fragmented neural arches (MAP-8511 and MAP-8513), which only preserve the base of the neural spine

and the postzygapophyses. The postzygapophyses are also elliptical but those of MAP-8513 are more subcircular. In addition, they are ventrolaterally directed and separated between them with an angle higher than 90 degrees (Figure S1 in Supplementary Data, File S1).

The most anterior vertebra MAP-8518 (probably the third) is longer and less high than the following MAP-8501 and MAP-8519 (possible fourth and sixth vertebrae, respectively) but resembles MAP-8494 (probably the eighth) in length and height (Supplementary Data, File S1). So, cervical vertebrae become shorter but higher towards the middle region and elongated again towards the posterior region. MAP-8494 displays a height similar to the most anterior vertebra MAP-8518, but this is because of distortion. Moreover, the degree of opisthocoely not only increases to the posterior region but, also, the ventral keel widens and the neural arches become higher and wider (Supplementary Data, File S1). In addition, the postzygapophyses change from a subcircular shape to sub-elliptical, being longer for subsequent positions (e.g., Figure 4L,X).

Dorsal vertebrae: Two vertebrae (MAP-8499 and MAP-8495) are regarded as anterior dorsals (Figure 5; Supplementary Data, File S1). Both vertebrae display slightly distorted and fragmented neural arches, though the centra are moderately well preserved. These centra are amphiplatyan (slightly platycoelous) (Figure 5A,G) and higher than long and wide (Figure 5C,I). While the anterior articular facets are elliptic (i.e., higher than wide in the cranial view, Figure 5A,G; Supplementary Data, File S1), posterior articular faces are more subcircular (i.e., almost as high as wide, Figure 5B,H; Supplementary Data, File S1). Lateral surfaces are markedly craniocaudally concave and dorsoventrally convex (Figure 5C,D,I,J); so, centra look highly constricted between articular faces which have everted margins, in part because of distortion. In the ventral view, both vertebrae have a longitudinal keel, which is more pronounced in MAP-8499 (Figure 5F) than in MAP-8495 (Figure 5L).

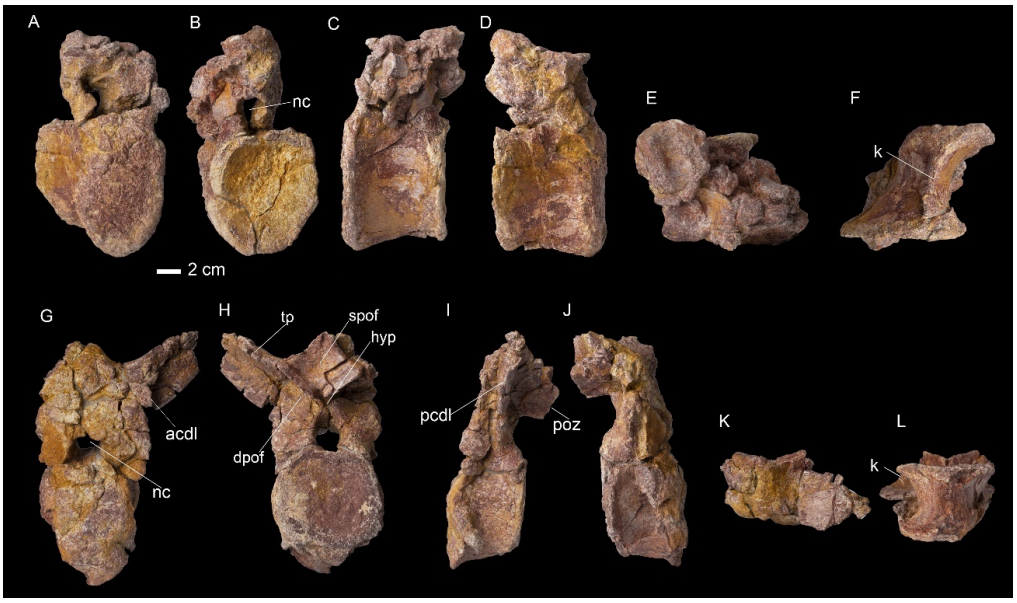

Figure 5. Dorsal vertebrae of the *I. galvensis* specimen from the SC-4 site (Galve, Teruel, Spain). (**A**–**F**), MAP-8499. (**G**–**L**), MAP-8495. Views: cranial (**A**,**G**), caudal (**B**,**H**), left lateral (**C**,**I**), right lateral (**D**,**J**), dorsal (**E**,**K**), and ventral (**F**,**L**). Abbreviations: acdl, anterior centrodiapophyseal lamina; nc, neural canal; dpof, diapopostzygapophyseal fossa; hyp, hyposphene; k, keel; pcdl, posterior centrodiapophyseal lamina; poz, postzygapophysis; spof, spinopostzygapophyseal fossa; tp, transverse process.

The neurocentral suture is sigmoid and closed in both vertebrae. The neural arch of MAP-8499 is incomplete, crushed and distorted, and covered by bone fragments, hiding the apophyses (Figure 5A,B). In contrast, MAP-8495 displays a neural arch with more visible structures, though prezygapophyses are not preserved. The neural canal in MAP-8495 is subcircular, higher than wide (Figure 5H; Supplementary Data, File S1). MAP-8495 does

not have preserved parapophyses, but it seems that, in the area of the left lateral, between the base of the transverse process and the vertebral centrum and both the anterior and the posterior centrodiapophyseal laminae, there is a concave area that could correspond to this structure (Figure 5I). The posterior lamina is more robust than the anterior one and runs along the preserved lateral surface from a more ventral position (Figure 5I). In the caudal view, this vertebra displays two fossae, a very concave and elliptical diapopostzygapophyseal fossa and another less accentuated and rhomboid spinopostzygapophyseal fossa (Figure 5H). A hyposphene is situated in the deeper region of the diapopostzygapophyseal fossa (Figure 5H). The postzygapophyses are flat and elliptic (longer than wide). The angle between the transverse processes (the proximal region of the left and the base of the right) is about 92°. In addition, MAP-8499 shows some fragments of tendons attached in the anterior region of the base of the neural spine (Figure 5E).

The presence of dorsal vertebrae with higher than long and wide centra, parapophyses that, although not well preserved, are presumably located at the region between the centrum and the transverse processes (and not in the transverse process such as in the middle to posterior dorsals), and an angle of 92° between the transverse processes is indicative that both vertebrae are anterior dorsals. MAP-8499 is longer and higher than MAP-8495, whereas MAP-8495 is wider and displays a wider ventral keel, so MAP-8499 is the most anterior vertebra (possibly the fourth or third), whereas MAP-8495 occupied a more posterior position in the dorsal series (potentially the fifth).

Caudal vertebrae: The caudal region is represented by an almost complete anterior caudal vertebra (MAP-8500), a well-preserved middle caudal centrum (MAP-4676), and four fragments of middle to posterior caudal centra (MAP-6899, MAP-6970, MAP-6972, and MAP-8510) (Figure 6; Supplementary Data, File S1). The most anterior vertebra (MAP-8500) has a platycoelous centrum (Figure 6A,B), which is higher than wide and large (Figure 6C,D). Articular facets are sub-rectangular and higher than wide (Supplementary Data, File S1). The lateral surfaces are craniocaudally concave and dorsoventrally convex (Figure 6C,D). The ventral surface is narrow and compressed between the wide chevron articular faces (Figure 6F).

The neural canal is narrow and circular (Figure 6A). The transverse processes are wide and they are in the most proximal region of the centrum and directed laterally (Figure 6C,D). The neurocentral suture is sigmoid and fully closed. The prezygapophyses are oval, larger than wide and inclined anteriorly, protruding forward of the anterior articular facet (Figure 6A). The postzygapophyses are subcircular and they are located at the base of the neural spine and separated between them by a shallow fossa. The neural spine is wide and robust, widening in its middle region, and posteriorly inclined (Figure 6C).

Regarding middle to posterior caudal vertebrae, MAP-4676 is the best-preserved example. This centrum is amphiplatyan (slightly platycoelous), with hexagonal articular faces (Figure 6I,J). The posterior articular face is more concave than the anterior one (Figure 6I–N). In the lateral view, this centrum is craniocaudally concave and dorsoventrally convex, with a slightly anteroposterior keel (Figure 6K,L). The neurocentral suture is also sigmoid and closed. In the ventral view, MAP-6899 displays a longitudinal ventral groove (Figure 6M). The chevron articular facet is proportionally longer in this middle caudal centrum than in the anterior of MAP-8500. The rest of the centra, that comprise the middle and posterior region, also have amphiplatyan centra with hexagonal anterior and posterior surfaces and a ventral groove but smaller (Figure 6O–Z).

Along the caudal series, the vertebrae display the main anatomical features of each region, from anterior caudal vertebrae anteroposteriorly compressed, which lengthen and decrease in width and height to the middle region, and then they decrease in all dimensions to the most posterior region, among other features.

Figure 6. Caudal vertebrae of the *I. galvensis* specimen from the SC-4 site (Galve, Teruel, Spain). (**A**–**F**), MAP-8500. (**G**,**H**), MAP-8510. (**I**–**N**), MAP-4676. (**O**–**T**), MAP-6972. (**U**,**V**), MAP-6970. (**W**–**Z**), MAP-6899. Views: cranial (**A**,**G**,**I**,**O**,**U**,**W**), caudal (**B**,**J**,**P**,**X**), left lateral (**C**,**K**,**Q**,**Y**), right lateral (**D**,**J**), dorsal (**E**,**K**), and ventral (**F**,**L**). Abbreviations: cf, chevron articular facet; nc, neural canal; g, ventral groove; ns, neurocentral suture; nsp, neural spine; poz, postzygapophysis; prz, prezygapophysis; tp, transverse process.

Cervical ribs: There are six cervical ribs, an anterior (atlas) and the other five more posterior (Figure 7; Supplementary Data, File S1). Apart from the atlas rib (MAP-6889 + MAP-6893), which is an elongated shaft (Figure 7A), all the consecutive cervical ribs have capitulum and tuberculum. If they have it preserved, they retain a large capitular process, larger than that of the capitulum. Both articular facets are oval and concave (Figure 7K,M). The rib shaft has a smooth and convex anterior surface, whereas the posterior surface is concave, which becomes more concave towards more posterior regions (Figure 7K). The cervical ribs lengthen towards the posterior region.

Figure 7. Cervical ribs of the *I. galvensis* specimen from the SC-4 site (Galve, Teruel, Spain). (**A**), MAP-6889 and MAP-6893. (**B**,**C**), MAP-8518. (**D**,**E**), MAP-8503. (**F**,**G**), MAP-.8507. (**H**,**I**), MAP-8502. (**J**,**K**), MAP-8519. (**L**,**M**), MAP-8514. Views: cranial (**A**,**B**,**D**,**F**,**H**,**J**,**L**) and caudal (**C**,**E**,**G**,**I**,**K**,**M**). Abbreviations: cap, capitulum; tu, tuberculum.

Dorsal ribs: MAP-8496 and MAP-8497 comprise two middle dorsal ribs (Figure 8). Both ribs share the same features, though MAP-8497 is shorter than MAP-8496 (Supplementary Data, File S1). The capitular process is perpendicular to the shaft of the rib and is longer in MAP-8496 than in MAP-8497 (Figure 8). The capitulum is rugose and oval (higher than wide) in the medial view. The tuberculum is more circular than the capitulum and lays in the beginning of the curvature of the shaft, where a cranial depression appears. The shaft is craniocaudally compressed, with an elliptic cross-section, and decreases in width distally. A prominent ridge rises at the caudal surface of the shaft of both ribs and extends from the base of the tuberculum to the most proximal third of the shaft, where it becomes less pronounced (Figure 8A,C).

Chevrons: Only an anterior complete chevron MAP-8516 is preserved (Figure 9; Supplementary Data, File S1). The proximal end is expanded transversely and composed of two articular facets. Each one is also divided unequally, with the anterior part larger than the posterior one (Figure 9A,C). The haemal canal is large but narrow. The shaft is proximodistally elongated but laterally compressed and first narrows but slightly expands distally. The distal end is elliptic and thin (Figure 9B).

Tendons: In addition to the two fragments of ossified tendons that lie on the anterior part of the neural arch of MAP-8499 (Figure 5A), there are several fragments of ossified tendons (MAP-8522). These elements are fibrous cylinders (Figure 10; Supplementary Data, File S1).

Scapula: MAP-8517 is an anterior fragment of the blade of a scapula (Figure 11; Supplementary Data, File S1). It is vastly crushed so it is little informative. The blade is

wide craniocaudally but thin transversally. In addition, it is (apparently) curved caudally (Figure 11A).

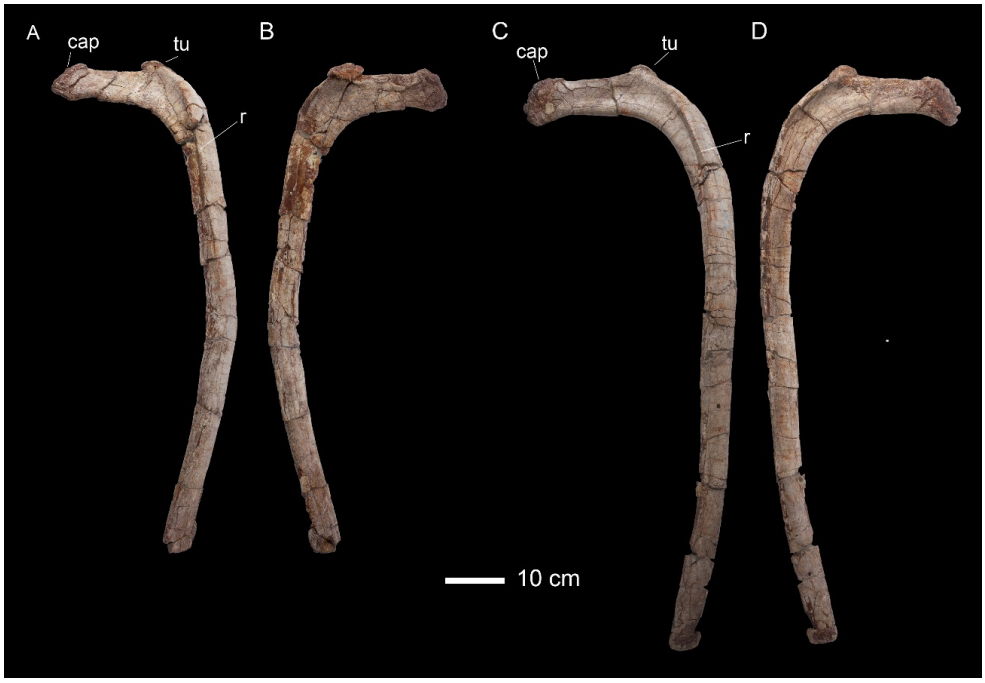

Figure 8. Dorsal ribs of the *I. galvensis* specimen from the SC-4 site (Galve, Teruel, Spain). (**A**,**B**), MAP-8496. (**C**,**D**), MAP-8497. Views: cranial (**A**,**C**) and caudal (**B**,**D**). Abbreviations: cap, capitulum; r, ridge; tu, tuberculum.

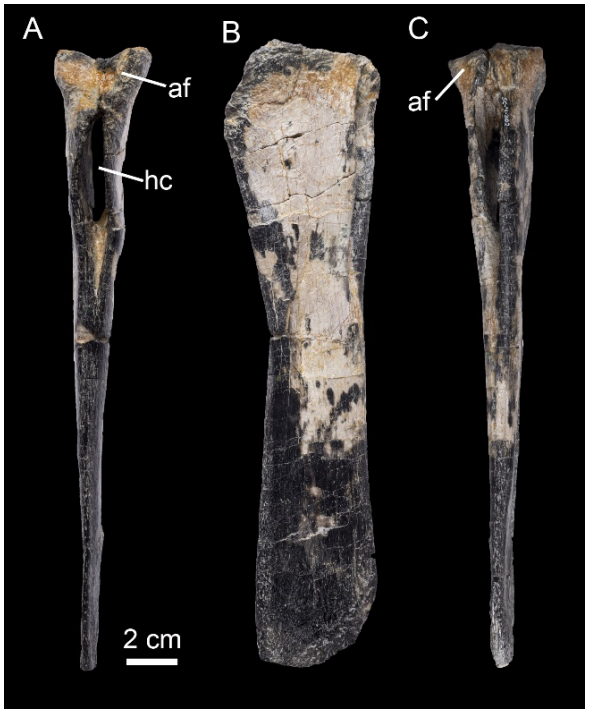

Figure 9. An anterior chevron MAP-8516 of the *I. galvensis* specimen from the SC-4 site (Galve, Teruel, Spain). Views: cranial (**A**), left lateral (**B**), and caudal (**C**). Abbreviations: af, articular facet; hc, haemal canal.

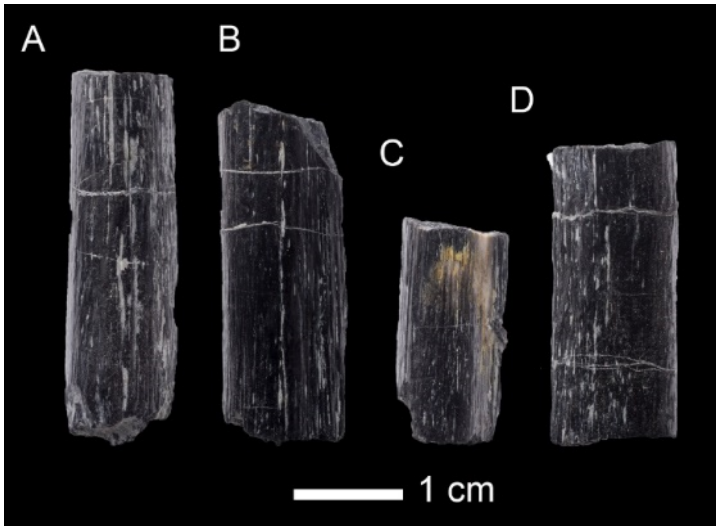

Figure 10. (**A**–**D**) Ossified tendons (MAP-8522) of the *I. galvensis* specimen from the SC-4 site (Galve, Teruel, Spain).

Figure 11. Fossils of the pectoral girdle of the *I. galvensis* specimen from the SC-4 site (Galve, Teruel, Spain). (**A**–**C**), A scapula MAP-8517. (**D**–**G**), two fragments of the right ulna MAP-8515. Views: lateral (**A**,**F**), dorsal (**B**), cranial (**D**), caudal (**E**), and medial (**C**,**G**). Abbreviations: c, crest.

Ulna: The right (?) ulna MAP-8515 is formed by two fragments with part of the diaphysis and the distal epiphysis (Figure 11; Supplementary Data, File S1). MAP-8515 is elongated, quite robust, and slightly rotates medially. The diaphysis is circular in cross-section and has a longitudinal ridge in the lateral view that extends down to the distal end (Figure 11F). The distal end is wider than the diaphysis and the articular face is oval and convex (Figure 11D).

Ischium: MAP-8498 is a massive, right ischium (Figure 12; Supplementary Data, File S1). The proximal region is constituted by both iliac and pubic peduncles, which form an almost right angle. The former is quadrangular in both lateral and medial views and larger and wider than the pubic peduncle. The articular surface is highly rugose and wide and displays a marked tuberosity located in its posterior half (Figure 12A,C). In contrast, the pubic peduncle is smaller, sub-rectangular in lateral and medial views, and has a less

rugose articular surface (Figure 12B). The peduncles are separated by the acetabulum, which is a sharp, deep, and semicircular concavity in the lateral view. The plate is flat to convex in the lateral view (Figure 12A), while it is flat in the ventral view (Figure 12B). Only the proximal part of the obturator process is preserved. The shaft is robust and has a "D" cross-section towards the distal end. The ischium shaft appears to have been straight in its preserved part and rotates cranially towards the most distal region.

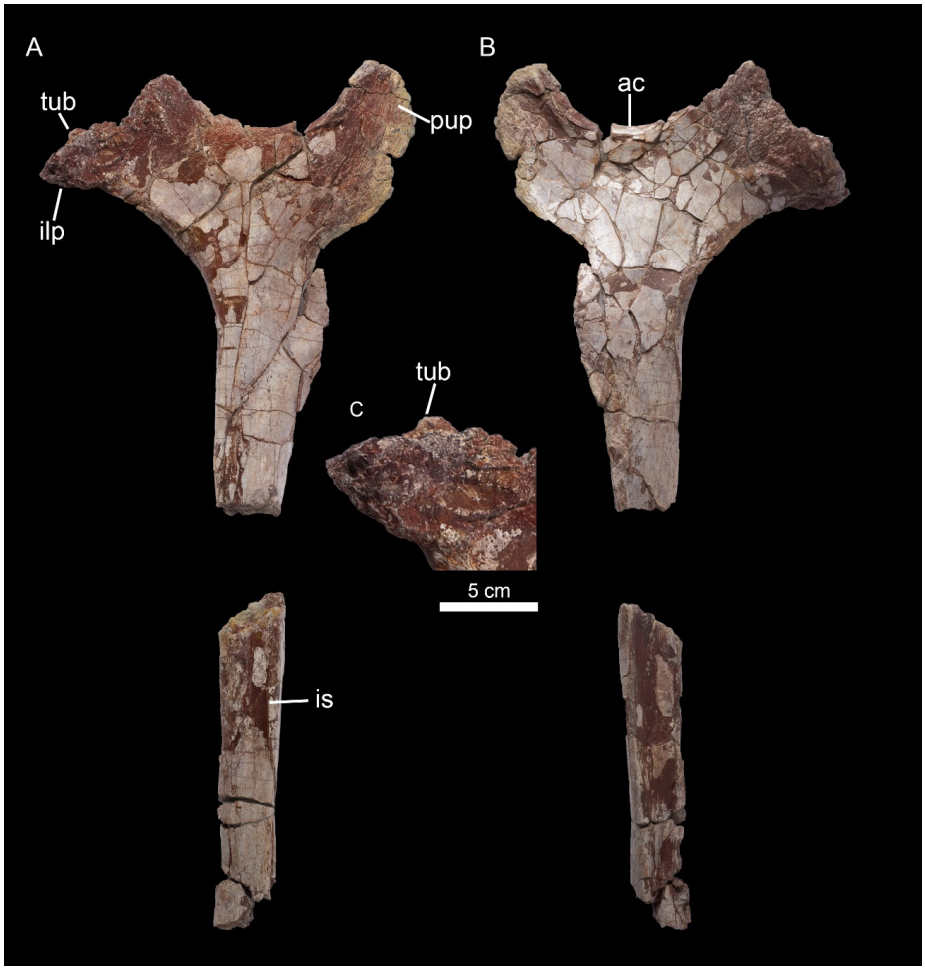

Figure 12. The partial right ischium MAP-8498 of the *I. galvensis* specimen from the SC-4 site (Galve, Teruel, Spain). Views: lateral (**A**) and medial (**B**). Detail of the tuberosity located at the iliac peduncle in lateral view (**C**). Abbreviations: ac, acetabulum; ilp, iliac peduncle; is, ischium shaft; pup, pubic peduncle; tub, tuberosity.

Tibia: MAP-8521 is a proximal epiphysis of the left tibia (Figure 13; Supplementary Data, File S1), which suffered a process of lateromedial crushing. As a result, it was flattened and broken in multiples fragments. Despite this, the cnemial crest and the fibular (or lateral) and inner (or medial) condyles can be observed at least partially. The proximal articular surface is rugose and convex (Figure 13C). The lateral surface is flat (probably due to deformation), while the lateral one is convex craniocaudally (Figure 13A,B). The cnemial crest is proportionally small, thin, and does not project much cranially. The fibular condyle has been partially eroded but it was smaller than the inner condyle, which was markedly more robust, and it is posteriorly directed. The intercondylar groove is observable and oblique in respect to the articular surface (Figure 13A).

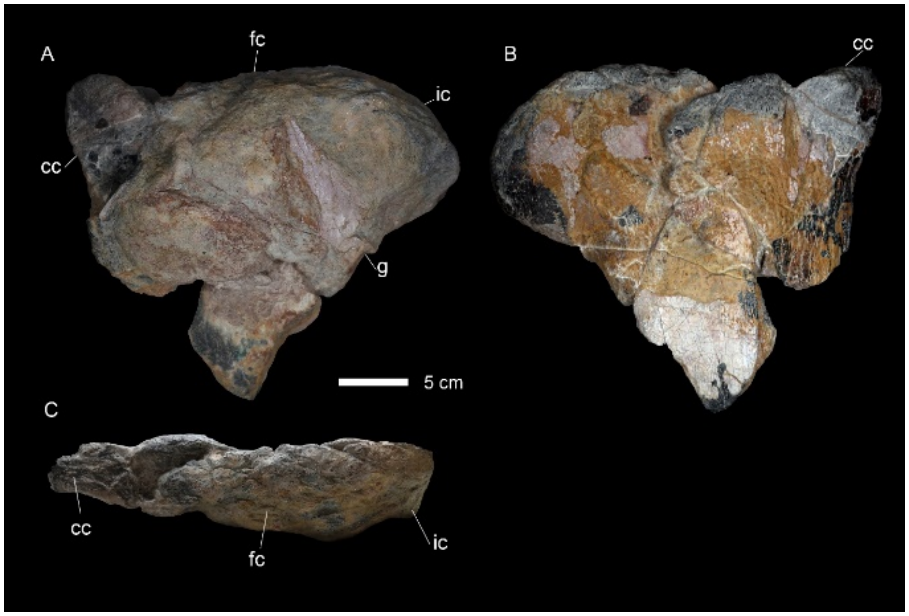

Figure 13. A proximal epiphysis MAP-8521 of the left tibia of the *I. galvensis* specimen from the SC-4 site (Galve, Teruel, Spain). Views: lateral (**A**), medial (**B**), and proximal (**C**). Abbreviations: cc, cnemial crest; fc, fibular condyle; ic, inner condyle; g, intercondylar groove.

Dubious material: MAP-8520 is probably a sternal (Figure 14; Supplementary Data, File S1). The fragment is composed of the craniomedial plate and caudolateral process. It is concave and flat in cranial and caudal views, respectively. The caudolateral process of MAP-8520 curves gently laterally (Figure 14A,B). MAP-8504 is a diaphysis of a long bone with an elliptical cross-section, interpreted here as part of the tibia (Figure 14D,E). MAP-8505 is probably a proximal fragment and a part of the plate of an ilium, perhaps the caudal end of the postacetabular process, which displays part of the brevis shelf (Figure 14F; Supplementary Data, File S1).

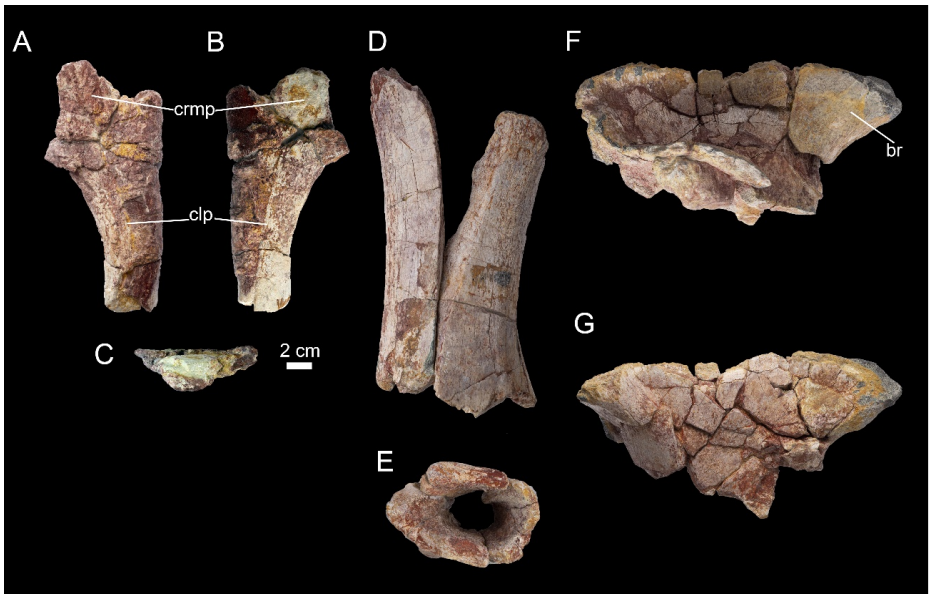

Figure 14. Dubious material of the *I. galvensis* specimen from the SC-4 site (Galve, Teruel, Spain). (**A**–**C**), Right sternal (?) MAP-8520. (**D**,**E**), Diaphysis MAP-8504 of a tibia (?). (**F**,**G**), Fragment of a plate of an ilium (?) MAP-8505. Views: lateral (**A**,**D**,**F**), medial (**B**,**G**), and proximal (**C**,**E**). Abbreviations: br, brevis shelf; clp, caudolateral process; crmp, craniomedial plate.

4.3. Results of the Morphometric Analysis

The resulting scatter plot for dorsal vertebrae is represented by two separated morphospaces of European Early Cretaceous iguanodontians (Figure 15), similar to results obtained by [20,34]. In the present analysis, the PC1 contributes 83.1 to the variance, in contrast to the 11.9 of PC2. PC1 greatly correlates with length and height but not with width. The sector with positive values of PC1 is occupied by robust taxa such as the *Iguanodon galvensis* from the SC-4 site, *Iguanodon* cf. *galvensis* (DS-1, CM-3, and CM-8), *Magnamanus* (MNS 2000/132, 2001/122, 2002/95, 2003/69, and 2004/54), and *I. bernissartensis* (RBINS R352 and CMP-MS-04). In contrast, the sector of negative values of PC1 is occupied by iguanodontians such as the slender *Valdosaurus* (IWCMS) and other larger ones such as *Mantellisaurus* (NHMUK R5764 and RBINS R57), a styracosternan related to *Morelladon* (CT-16 and CT-17), a tall-spined iguanodontian (GPIT 1802), *Morelladon* (CMP-MS-03-10), and *Brighstoneus* (MIWG 6344).

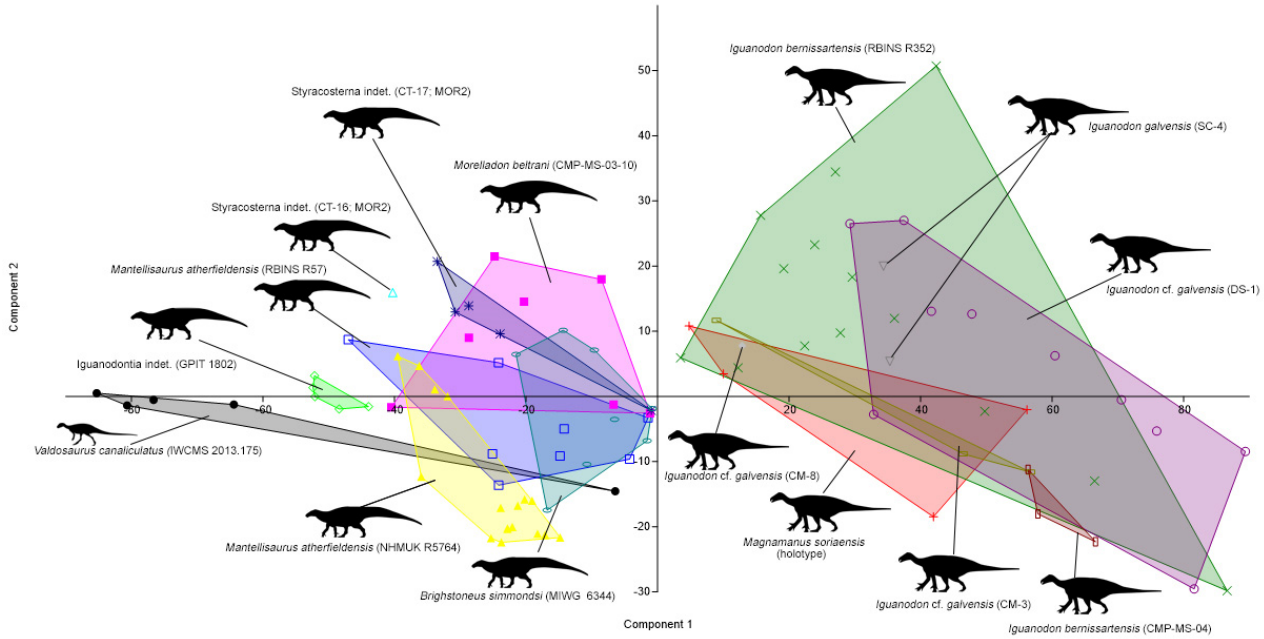

Figure 15. Scatter plot of the PCA of some iguanodontian dorsal vertebrae. Silhouettes were obtained from www.phylopic.org for *Mantellisaurus*, from [73] for *I. bernissartensis*, and modified from the reconstruction of *Hypsilophodon* made by [73] for *Valdosaurus*.

5. Discussion

5.1. Size and Ontogenetic Development

Skeletal maturity can be inferred based on several indicators such as body size, the neurocentral suture fusion (neurocentral synchondrosis), and the degree of postcranial co-ossification, among others [83]. Regarding dimensions of the material of the *Iguanodon galvensis* from the SC-4 site, some elements display a large and robust size. In fact, the third caudal vertebra MAP-8500 is comparable in length (87 mm) and height (132 mm) to the third caudal vertebra of the type specimen of *I. bernissartensis* (87 mm and 140 mm, respectively; RBINS R51 [7,8]) estimated as 8–10 m long [84]. In addition, the fourth dorsal vertebra MAP-8499 resembles in length (94 mm) and height (138 mm) the fifth dorsal vertebrae of a fully mature specimen of *I.* cf. *galvensis* (98 mm and 124 mm, respectively; DS-1) of 9–10 m long [21]. Moreover, all vertebral centra display a closed neurocentral suture, most likely indicating that SC-4 specimen was a mature specimen, as occurs in some groups of sauropsids, such as crocodylians (e.g., [85,86]) and some ornithopods [87,88]. In addition, the large specimen of the SC-4 site displays some cervical ribs fused to their corresponding vertebrae (Figure 4). Co-ossification between adjacent non-sacral vertebrae and between these vertebrae and their corresponding ribs have been less documented than in the case of

the sacral vertebrae for ornithopods and many other reptiles (e.g., [83,89–92]). Despite this, costovertebral fusion has been observed in the fully mature holotype of "*Delapparentia*" (in cervical vertebrae, pers. obs. V2 447 and dorsal vertebrae, [33]), an advanced-aged specimen of *Iguanodon* cf. *galvensis* (in dorsal vertebrae, [21]), *Ouranosaurus* (in cervical vertebrae, [93]), *Brachylophosaurus* (in cervical vertebrae, [94]), *Edmontosaurus regalis* (in cervical vertebrae, [95]), and *Olorotitan* (in cervical vertebrae, [96]). Therefore, considering the three criteria discussed above, the specimen from the SC-4 site was a large (around 10 m long), robust, and likely skeletally mature individual of *Iguanodon galvensis*.

5.2. Clade Affinities of the SC-4 Specimen

The presence of vertebral centra without pleurocoeli, dorsal and caudal vertebral centra slightly compressed anteroposteriorly, and middle caudal centra with hexagonal contour and sinuous neurocentral suture demonstrate ornithopod affinities for the SC-4 specimen (e.g., [20,30,97,98]). Within Ornithopoda, caudal vertebrae with hexagonal articular facets are typical in iguanodontians such as in the SC-4 specimen (Figure 6) and unlike in hypsilophodontids [98]. In addition, the fossils of the SC-4 specimen clearly differ from those of rhabdodontomorphans and dryosaurids in size. Moreover, the presence of highly opisthocoelous centra in the cervical vertebrae (Figure 4) is diagnostic of the Styracosterna clade sensu [12]. In addition, the maxillary crown MAP-8523 displays a primary ridge distally offset in the labial surface (Figure 3), like non-hadrosaurid iguanodontians (e.g., [12,19,99–101]). Therefore, SC-4 specimen is referred to a non-hadrosaurid styracosternan.

5.3. Comparison with Other Early Cretaceous Styracosternans

Herein, only those well-preserved fossils of the SC-4 styracosternan are compared with Early Cretaceous styracosternans from Europe.

Highly opisthocoelous and ventrally keeled cervical vertebrae (Figure 4) are a widespread feature among styracosternans [12]. This is the case of European taxa such as *Barilium* [9], *Hypselospinus* [10,12], *Magnamanus* [25], *Iguanodon* cf. *galvensis* [31,34], *I. bernissartensis* [7], *Mantellisaurus* [8,24], and *Proa* (e.g., AR-1/103). Cervical vertebrae in *Morelladon* and *Brighstoneus* are unknown [16,22].

The anterior dorsal vertebrae MAP-8495 and MAP-8499 have amphiplatyan centra with elliptical (higher than wide) articular facets such as the dorsal vertebrae of *Hypselospinus* [10,12], *Barilium* [9], *Iguanodon* cf. *galvensis* [21], I. *bernissartensis* [7], *Mantellisaurus* [8,24], and *Brighstoneus* [22], in contrast to the platycoelous dorsal vertebrae of *Morelladon* [16]. In addition, these vertebrae are markedly higher than long and wide, like in *Hypselospinus* [10,12], *Barilium* [9], *Magnamanus* [25], *Iguanodon* cf. *galvensis* [21], and *I. bernissartensis* [7]. This is different to longer than high centra (or as high as long) in *Mantellisaurus* [8,24], *Morelladon* [16], and *Brighstoneus* [22]. Dorsal vertebrae of the SC-4 specimen have a longitudinal ventral keel such as in the anterior ones of *Hypselospinus* [10,12], *I. galvensis* [21,26], *I. bernissartensis* [7], *Mantellisaurus* [8,24], and *Brighstoneus* [22]. Moreover, centra of MAP-8495 and MAP-8499 are markedly compressed between the anterior and posterior articulations so their margins are everted, as in the anterior dorsal vertebrae of *Iguanodon galvensis* [21,26] and *I. bernissartensis* [7,17,26] but unlike the craniocaudally expanded dorsals of *Mantellisaurus* [8], *Morelladon* [16], and *Brighstoneus* [22]. On the other hand, PCA also reflects that both MAP-8495 and MAP-8499 vertebrae are more like large taxa such as *Magnamanus* and *Iguanodon* spp. than those of more lightly built *Mantellisaurus*, *Morelladon*, or *Brighstoneus* (Figure 15). In particular, dorsal series in *I. galvensis* are represented by anterior keeled and moderately compressed anteroposterior vertebrae and middle and posterior dorsal vertebrae with a smooth ventral surface but also with slight compression. In contrast, *I. bernissartensis* has keeled and highly compressed dorsal vertebrae. Anterior dorsal vertebrae are unknown in *Barilium* [9], *Magnamanus* [25], and *Morelladon* [16], so direct comparison with these taxa cannot be well contrasted.

The most anterior caudal vertebra MAP-8500 is platycoelous with sub-quadrangular articular faces, such as in *Hypselospinus* [10,12], *Magnamanus* [25], *Iguanodon* cf. *galvensis* [34],

Iguanodon bernissartensis [7,17], and, apparently, in *Brighstoneus* [22], in contrast to the amphiplatyan ones of *Barilium* [9] and *Mantellisaurus* [8,24]. The caudal region of *Morelladon* is unknown [16]. In contrast, middle to posterior caudal vertebrae of the SC-4 specimen closely resemble those of other styracosternans in terms of the presence or absence of a ventral groove and the shape and contour of the articular faces (e.g., [17,22,33–35,102,103]).

The preserved parts of the ulna MAP-8515 do not differ much to that of *Magnamanus* [25], *I. bernissartensis* (Figure 58 in [7]), or *Mantellisaurus* [24].

The iliac peduncle of the right ischium MAP-8498 (Figure 16A) is proportionally more massive than the pubis peduncle such as in *Hypselospinus* (Figure 16B) [10], *I. galvensis* (Figure 16C) [26], *I. bernissartensis* (Figure 16D) [7], and *Morelladon* (Figure 16F) [16], unlike those more similar in proportions of *Barilium* (Figure 16I) [9], "*Delapparentia*" (Figure 16G) [32] and, apparently, *Brighstoneus* (Figure 16H) [22]. The angle between both peduncles is more accentuated in *I. galvensis* (Figure 16C) [26], *I. bernissartensis* (Figure 16D) [26], and, possibly, in *Morelladon* [16]. In addition, MAP-8498 displays a prominent tuberosity in the dorsal surface of the iliac peduncle (Figure 12C), as it has been described as autapomorphic of *I. galvensis* [26]. This feature is absent in the European *I. bernissartensis* [7], *Brighstoneus* [22], and *Morelladon* [16]. The deep, sharp, and semicircular margin of the acetabulum resembles also not only those of *Iguanodon* spp. (Figure 16C,D) [26] but *Morelladon* (Figure 16F) [16], and it is unlike the British styracosternans *Barilium* (Figure 16I) [9] and *Hypselospinus* (Figure 16B) [10,12]. The ischiatic shaft seems to be straight as in *Mantellisaurus* (Figure 16E) or *Morelladon* (Figure 16F), but this trait was individually variable in *Iguanodon* [19]. The ischiatic shaft of MAP-8498 is D-shaped in cross-section as in *I. galvensis* [26], whereas it is triangular in *I. bernissartensis* [26] and *Brighstoneus* [22].

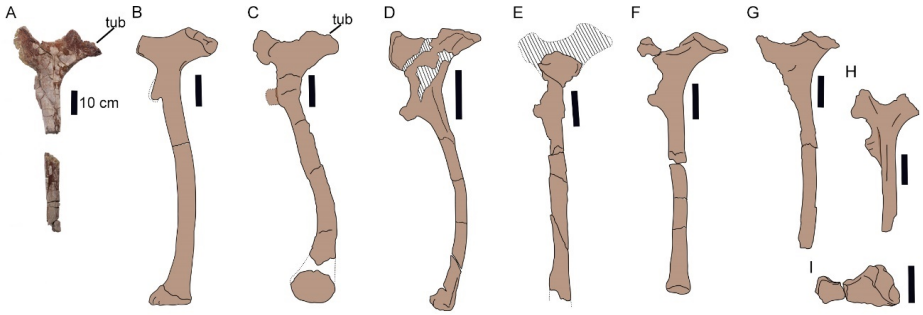

Figure 16. Ischia of some European styracosternans from the Early Cretaceous. (**A**), MAP- 8498. (**B**), Ischium of *Hypselospinus*, redrawn from [10]. (**C**), Ischium of *I. galvensis*, redrawn from [26]. (**D**), Ischium of *I. bernissartensis*, redrawn from [7]. (**E**), Ischium of *Mantellisaurus*, redrawn from [8]. (**F**), Ischium of *Morelladon*, redrawn from [16]. (**G**), Ischium of '*Delapparentia*', redrawn from [32]. (**H**), Ischium of *Brighstoneus*, redrawn from [22]. (**I**), Ischium of *Barilium*, redrawn from [9]. Abbreviations: tub, tuberosity. Scales equal 10 cm.

To sum up, the combination of (1) amphiplatyan, (2) higher than long, and (3) markedly transversely compressed anterior dorsal centra, (4) platycoelous anterior caudal vertebrae, and (5) a larger iliac peduncle than the pubic and (6) deep acetabulum in the ischium suggest affinities with *Magnamanus* and *Iguanodon* spp., as is also apparent from the PCA. Nevertheless, the presence of a (1) marked tuberosity over the iliac peduncle and a (2) D-shaped cross-section of the ischiatic shaft are diagnostic of *I. galvensis* [26]. Thus, the SC-4 specimen is, here, assigned to *Iguanodon galvensis.*

6. Conclusions

The osteological fossils of a massively constructed ornithopod from the SC-4 site in facies of the lower Barremian (Lower Cretaceous) Camarillas Formation of Galve have been described. The presence of fused cervical vertebrae and ribs and closed neurocentral suture indicate that it was a fully mature individual. In addition, the extraordinary dimensions

of some fossils reveal that it was a large (around 10 m) and robust specimen. Although most of the osteological fossils resemble large taxa such as *Magnamanus* and *Iguanodon* spp. in some anatomical features mainly in the vertebrae, the presence of a (1) marked tuberosity over the iliac peduncle and a (2) D-shaped cross-section of the ischiatic shaft are diagnostic of *I. galvensis*. The use of principal component analysis applied over dorsal vertebrae demonstrates again that this method is very useful to discriminate whether the ornithopod taxon is of one morphotype (robust and large-sized) or another (slender and medium-sized). In fact, SC-4 vertebrae fall into the morphospace of large and robust related forms like *Iguanodon* spp. and *Magnamanus*, which support its classification to *Iguanodon galvensis*. The study of this specimen increases the osteological knowledge of adults of this species and reinforces the previous diagnosis for this taxon with more fossil evidence.

Supplementary Materials: The following supporting information can be downloaded at: https://www.mdpi.com/article/10.3390/d16090586/s1. Supplementary Data, File S1. Additional information about the SC-4 material. Supplementary Data, File S2. Data matrix of vertebrae measurements of several ornithopods.

Author Contributions: Conceptualization, J.G.-C., F.J.V. and A.C.; methodology, J.G.-C., F.J.V. and A.C.; validation, F.J.V. and A.C.; formal analysis, J.G.-C., F.J.V. and A.C.; investigation, J.G.-C., F.J.V. and A.C.; resources, J.G.-C., F.J.V. and A.C.; data curation, J.G.-C. and F.J.V.; writing—original draft preparation, J.G.-C.; writing—review and editing, F.J.V. and A.C.; supervision, F.J.V. and A.C.; project administration, A.C.; funding acquisition, A.C. All authors have read and agreed to the published version of the manuscript.

Funding: This research was funded by the Gobierno de Aragón (Spain) through the Research Group E04_23R FOCONTUR, the Instituto Aragonés de Fomento, and Unidad de Paleontología de Teruel (Ministerio de Ciencia, Innovación y Universidades, Gobierno de España).

Institutional Review Board Statement: Not applicable.

Data Availability Statement: All data and material are available for other research. Fossils of the SC-4 specimen are housed at Museo Aragonés de Paleontología.

Acknowledgments: The authors would like to thank PAMESA Cerámica Compacto S.L.U. (previously SIBELCO Minerales Cerámicos S.A.) for its logistic help in the clay mine. In addition, we are also grateful to the colleagues from the Fundación Conjunto Paleontológico de Teruel-Dinópolis (Teruel, Spain) for their support throughout these years. Finally, we also appreciate useful comments and suggestions made by the Assistant Editor and the three anonymous reviewers.

Conflicts of Interest: The authors declare no conflicts of interest.

References

1. Huxley, T.H. On *Hypsilophodon foxii*, a new dinosaurian from the Wealden of the Isle of Wight. *Q. J. Geol. Soc.* **1870**, *26*, 3–12.
2. Galton, P.M. The ornithischian dinosaur *Hypsilophodon* from the Wealden of the Isle of Wight. *Bull. Br. Mus. (Nat. Hist.) Geol.* **1974**, *25*, 1–152.
3. Ruiz-Omeñaca, J.I.; Canudo, J.I.; Cuenca-Bescós, G.; Cruzado-Caballero, P.; Gasca, J.M.; Moreno-Azanza, M. A new basal ornithopod dinosaur from the Barremian of Galve, Spain. *Comptes Rendus Palevol* **2012**, *11*, 435–444.
4. Longrich, N.R.; Martill, D.M.; Munt, M.; Green, M.; Penn, M.; Smith, S. *Vectidromeus insularis*, a new hypsilophodontid dinosaur from the Lower Cretaceous Wessex Formation of the Isle of Wight, England. *Cretac. Res.* **2024**, *154*, 105707.
5. Dieudonne, P.E.; Tortosa, T.; Torcida Fernandez-Baldor, F.; Canudo, J.I.; Diaz-Martinez, I. An unexpected early rhabdodontid from Europe (Lower Cretaceous of Salas de los Infantes, Burgos Province, Spain) and a re-examination of basal iguanodontian relationships. *PLoS ONE* **2016**, *11*, e0156251.
6. Galton, P.M. Dinosaurs (Reptilia: Ornithischia). *Palaeontol.* **1975**, *18*, 741–752.
7. Norman, D.B. On the ornithischian dinosaurs *Iguanodon bernissartensis* from the Lower Cretaceous of Bernissart (Belgium). *Bull. Inst. Sci. Nat. Belg. Mémories* **1980**, *178*, 1–104.
8. Norman, D.B. On the anatomy of *Iguanodon atherfieldensis* (Ornithischia: Ornithopoda). *Bull. Inst. Sci. Nat. Belg. Sci. Terre* **1986**, *56*, 281–372.
9. Norman, D.B. On the osteology of the lower Wealden (Valanginian) ornithopod *Barilium dawsoni* (Iguanodontia: Styracosterna). *Spec. Pap. Palaeontol.* **2011**, *86*, 165–194.

10. Norman, D.B. Ornithopod dinosaurs. In *Field guide to the Wealden of England*; Batten, D.J., Ed.; The Palaeontological Association: Oxford, UK, 2011; pp. 407–475.
11. Norman, D.B. Iguanodontian taxa (Dinosauria: Ornithischia) from the Lower Cretaceous of England and Belgium. In *Bernissart Dinosaurs and Early Cretaceous Terrestrial Ecosystems*; Godefroit, P., Ed.; Indiana University Press: Bloomington, IN, USA, 2012; pp. 175–212.
12. Norman, D.B. On the history, osteology, and systematic position of the Wealden (Hastings group) dinosaur *Hypselospinus fittoni* (Iguanodontia: Styracosterna). *Zool. J. Linn. Soc.* **2015**, *173*, 92–189.
13. Mcdonald, A.T.; Espilez, E.; Mampel, L.; Kirkland, J.I.; Alcalá, L. An unusual new basal iguanodont (Dinosauria: Ornithopoda) from the Lower Cretaceous of Teruel, Spain. *Zootaxa* **2012**, *3595*, 61–76.
14. Serrano, M.L.; Vullo, R.; Marugán-Lobón, J.; Ortega, F.; Buscalioni, A.D. An articulated hindlimb of a basal iguanodont (Dinosauria, Ornithopoda) from the Early Cretaceous Las Hoyas Lagerstätte (Spain). *Geol. Mag.* **2013**, *150*, 572–576. [CrossRef]
15. Gasulla, J.M.; Escaso, F.; Ortega, F.; Sanz, J.L. New hadrosauriform cranial remains from the Arcillas de Morella Formation (lower Aptian) of Morella, Spain. *Cretac. Res.* **2014**, *47*, 19–24. [CrossRef]
16. Gasulla, J.M.; Escaso, F.; Narváez, I.; Ortega, F.; Sanz, J.L. A new sail-backed styracosternan (Dinosauria: Ornithopoda) from the Early Cretaceous of Morella, Spain. *PLoS ONE* **2015**, *10*, e0144167. [CrossRef]
17. Gasulla, J.M.; Escaso, F.; Narváez, I.; Sanz, J.L.; Ortega, F. New *Iguanodon bernissartensis* Axial Bones (Dinosauria, Ornithopoda) from the Early Cretaceous of Morella, Spain. *Diversity* **2022**, *14*, 63. [CrossRef]
18. Verdú, F.J.; Royo-Torres, R.; Cobos, A.; Alcalá, L. Perinates of a new species of *Iguanodon* (Ornithischia: Ornithopoda) from the lower Barremian of Galve (Teruel, Spain). *Cretac. Res.* **2015**, *56*, 250–264. [CrossRef]
19. Verdú, F.J.; Godefroit, P.; Royo-Torres, R.; Cobos, A.; Alcalá, L. Individual variation in the postcranial skeleton of the Early Cretaceous *Iguanodon bernissartensis* (Dinosauria: Ornithopoda). *Cretac. Res.* **2017**, *74*, 65–86. [CrossRef]
20. Verdú, F.J.; Cobos, A.; Royo-Torres, R.; Alcalá, L. Diversity of large ornithopod dinosaurs in the Upper Hauterivian-Lower Barremian (Lower Cretaceous) of Teruel (Spain): A morphometric approach. *Span. J. Palaeontol.* **2021**, *34*, 269–288. [CrossRef]
21. Verdú, F.J.; Royo-Torres, R.; Cobos, A.; Alcalá, L. Systematics and paleobiology of a new articulated axial specimen referred to *Iguanodon* cf. *galvensis* (Ornithopoda, Iguanodontoidea). *J. Vertebr. Paleontol.* **2020**, *40*, e1878202. [CrossRef]
22. Lockwood, J.A.F.; Martill, D.M.; Maidment, S.C.R. A new hadrosauriform dinosaur from the Wessex Formation, Wealden Group (Early Cretaceous), of the Isle of Wight, southern England. *J. Syst. Palaeontol.* **2021**, *19*, 847–888. [CrossRef]
23. Santos-Cubedo, A.; de Santisteban, C.; Poza, B.; Meseguer, S. A new styracosternan hadrosauroid (Dinosauria: Ornithischia) from the Early Cretaceous of Portell, Spain. *PLoS ONE* **2021**, *16*, e0253599.
24. Bonsor, J.A.; Lockwood, J.A.; Leite, J.V.; Scott-Murray, A.; Maidment, S.C. The osteology of the holotype of the british iguanodontian dinosaur *Mantellisaurus atherfieldensis*. *Monogr. Palaeontogr. Soc.* **2023**, *177*, 1–63.
25. Fuentes-Vidarte, C.; Meijide-Calvo, M.; Meijide-Fuentes, F.; Meijide-Fuentes, M. Un nuevo dinosaurio estiracosterno (Ornithopoda: Ankylopollexia) del Cretácico Inferior de España. *Span. J. Palaeontol.* **2016**, *31*, 407–446.
26. Verdú, F.J.; Royo-Torres, R.; Cobos, A.; Alcalá, L. New systematic and phylogenetic data about the early Barremian *Iguanodon galvensis* (Ornithopoda: Iguanodontoidea) from Spain. *Historical Biol.* **2018**, *30*, 437–474.
27. Lapparent, A.F. and Zbyszewski, G. Les dinosauriens du Portugal. *Mern. Serv. Geol. Port.* **1957**, *2*, 1–63.
28. Figueiredo, S.D.; Rosina, P.; Figuti, L. Dinosaurs and other vertebrates from the Papo-Seco Formation (Lower Cretaceous) of southern Portugal. *J. Iber. Geol.* **2015**, *41*, 301–314.
29. Figueiredo, S.D.; de Souza Carvalho, I.; Pereda-Suberbiola, X.; Cunha, P.P.; Strantzali, I.B.; Antunes, V. Ornithopod dinosaur remains from the Papo Seco Formation (lower Barremian, Lusitanian Basin, Portugal): A review of old and new finds. *Hist. Biol.* **2023**, *35*, 2181–2192. [CrossRef]
30. Pereda-Suberbiola, X.; Ruiz-Omenaca, J.I.; Fernández-Baldor, F.T.; Maisch, M.W.; Huerta, P.; Contreras, R.; Izquierdo, L.Á.; Montero Huerta, D.; Urién Montero, V.; Welle, J. A tall-spined ornithopod dinosaur from the Early Cretaceous of Salas de los Infantes (Burgos, Spain). *Comptes Rendus Palevol* **2011**, *10*, 551–558.
31. Sanguino, F.; Buscalioni, Á.D. The *Iguanodon* locality of Pata la Mona (upper Barremian, Buenache de la Sierra, Cuenca) revisited. In Proceedings of the XVI Encuentro de Jóvenes Investigadores en Paleontología, Zarautz, Spain, 11–14 April 2018; pp. 11–14.
32. Gasca, J.M.; Canudo, J.I.; Moreno-Azanza, M. On the diversity of Iberian iguanodont dinosaurs: New fossils from the lower Barremian, Teruel province, Spain. *Cretac. Res.* **2014**, *50*, 264–272.
33. Gasca, J.; Moreno-Azanza, M.; Ruiz-Omeñaca, J.I.; Canudo, J.I. New material and phylogenetic position of the basal iguanodont dinosaur *Delapparentia turolensis* from the Barremian (Early Cretaceous) of Spain. *J. Iber. Geol.* **2015**, *41*, 57–70.
34. García-Cobeña, J.; Verdú, F.J.; Cobos, A. Abundance of large ornithopod dinosaurs in the El Castellar Formation (Hauterivian–Barremian, Lower Cretaceous) of the Peñagolosa sub-basin (Teruel, Spain). *J. Iber. Geol.* **2022**, *48*, 107–127. [CrossRef]
35. García-Cobeña, J.; Cobos, A.; Verdú, F.J. Ornithopod tracks and bones: Paleoecology and an unusual evidence of quadrupedal locomotion in the Lower Cretaceous of eastern Iberia (Teruel, Spain). *Cretac. Res.* **2023**, *144*, 105473. [CrossRef]
36. Salas, R.; Guimerà, J. Rasgos estructurales principales de la cuenca Cretácica Inferior del Maestrazgo (Cordillera Ibérica oriental). *Geogaceta* **1996**, *20*, 1704–1706.
37. Díaz-Molina, M.; Yébenes, A. La sedimentación litoral y continental durante el Cretácico Inferior. *Estud. Geol.* **1987**, *43*, 3–21.

38. Salas, R.; Guimerà, J.; Mas, R.; Martín-Closas, C.; Meléndez, A.; Alonso, A. Peri-Tethys Memoir 6: Peri-Tethyan Rift/Wrench Basins and passive margins. In *Mémoires du Muséum National d'Histoire Naturelle*; Ziegler, P.A., Cavazza, W., Robertson, A.F.H., Crasquin-Soleau, S., Eds.; National Museum of Natural History: Paris, France, 2001; pp. 145–185.
39. Canérot, J.; Cugny, P.; Pardo, G.; Salas, R.; Villena, J. Ibérica Central y Maestrazgo. In *El Cretácico de España*; García, A., Ed.; Universidad Complutense de Madrid: Madrid, Spain, 1982; pp. 273–344.
40. Salas, R. El Malm i el Cretaci Inferior Entre el Massif de Garraf i la SERRA d'Espadà. Anàlisi de Conca. Ph.D. Thesis, Universidad de Barcelona, Barcelona, Spain, 1987.
41. Soria, A.R.; Liesa, C.L.; Navarrete, R.; Rodríguez-López, J.P. Sedimentology and stratigraphic architecture of Barremian synrift barrier island–estuarine depositional systems from blended field and drone-derived data. *Sedimentology* **2023**, *70*, 1812–1855. [CrossRef]
42. Soria, A.R. La Sedimentación en las Cuencas Marginales del Surco Ibérico Durante el Cretácico Inferior y su Control Tectónico. Ph.D. Thesis, Universidad de Zaragoza, Zaragoza, Spain, 1997.
43. Navarrete, R.; Rodríguez-López, J.P.; Liesa, C.L.; Soria, A.R.; Veloso, F.M. Changing physiography of rift basins as a control on the evolution of mixed siliciclastic carbonate back-barrier systems (Barremian Iberian Basin, Spain). *Sediment. Geol.* **2013**, *289*, 40–61.
44. Martín-Closas, C. Els Carofits del Cretaci Inferior de les Conques Periferiques del Bloc de l'Ebre. Ph.D. Thesis, Universidad de Barcelona, Barcelona, Spain, 1989.
45. Bover-Arnal, T.; Moreno-Bedmar, J.A.; Frijia, G.; Pascual-Cebrian, E.; Salas, R.S.R. Chronostratigraphy of the Barremian-Early Albian of the Maestrat Basin (E Iberian Peninsula): Integrating strontium-isotope stratigraphy and ammonoid biostratigraphy. *Newsl. Stratigr.* **2016**, *49*, 41–68.
46. Villanueva-Amadoz, U.; Sender, L.M.; Royo-Torres, R.; Verdú, F.J.; Pons, D.; Alcalá, L.; Diez, J.B. Palaeobotanical remains associated with dinosaur fossils from the Camarillas Formation (Barremian) of Galve (Teruel, Spain). *Hist. Biol.* **2015**, *27*, 374–388.
47. Schudack, U.; Schudack, M. Ostracod biostratigraphy in the Lower Cretaceous of the Iberian chain (eastern Spain). *J. Iber. Geol.* **2009**, *35*, 141–168.
48. Liesa, C.L.; Soria, A.R.; Casas, A.; Aurell, M.; Meléndez, N.; Bádenas, B.; Fregenal-Martínez, M.; Navarrete, R.; Peropadre, C.; Rodríguez- López, J.P. The South-Iberian, Central Iberian and Maestrazgo Basins. In *The Geology of Iberia: A Geodynamic Approach*; Quesada, C., Oliveira, J.T., Eds.; Springer Nature: Berlin/Heidelberg, Germany, 2019; Volume 3, pp. 214–228.
49. Royo-Torres, R.; Upchurch, P.; Mannion, P.D.; Mas, R.; Cobos, A.; Gascó, F.; Alcalá, L.; Sanz, J.L. The anatomy, phylogenetic relationships, and stratigraphic position of the Tithonian-Berriasian Spanish sauropod dinosaur *Aragosaurus ischiaticus*. *Zool. J. Linn. Soc* **2014**, *171*, 623–655.
50. Campos-Soto, S.; Benito, M.I.; Cobos, A.; Caus, E.; Quijada, I.E.; Suarez-González, P.; Mas, R.; Royo-Torres, R.; Alcalá, L. Revisiting the age and palaeoenvironments of the Upper Jurassic–Lower Cretaceous? dinosaur-bearing sedimentary record of eastern Spain: Implications for Iberian palaeogeography. *J. Iber. Geol.* **2019**, *45*, 471–510. [CrossRef]
51. Cobos, A.; Gascó, F. Presencia del icnogénero *Iguanodontipus* en el Cretácico Inferior de la provincia de Teruel (España). *Geogaceta* **2012**, *52*, 185–188.
52. Herrero-Gascón, J.; Pérez-Lorente, F. Nuevas aportaciones icnológicas de Galve (Teruel, España). Grandes huellas ornitópodas en el yacimiento de Santa Bárbara. *Geogaceta* **2013**, *53*, 21–24.
53. Royo-Torres, R.; Mampel, L.; Alcalá, L. Icnitas de dinosaurios del yacimiento San Cristóbal 3 de la Formación Camarillas en Galve (Teruel, España). *Geogaceta* **2013**, *53*, 5–8.
54. Navarrete, R.; Liesa, C.L.; Castanera, D.; Soria, A.R.; Rodríguez-López, J.P.; Canudo, J.I. A thick Tethyan multi-bed tsunami deposit preserving a dinosaur megatracksite within a coastal lagoon (Barremian, eastern Spain). *Sediment. Geol.* **2014**, *313*, 105–127.
55. Cobos, A.; Gasco, F.; Royo-Torres, R.; Lockley, M.G.; Alcalá, L. Dinosaur tracks as 'four-dimensional phenomena'reveal how different species moved. In *Dinosaur Tracks: The Next Steps*; Falkingham, P.L., Marty, D., Ritcher, A., Eds.; Indiana University Press: Bloomington and Indianapolis, IN, USA, 2016; pp. 244–256.
56. García-Cobeña, J.; Castanera, D.; Verdú, F.J.; Cobos, A. Diversity and discrimination of large ornithopods revealed through their tracks (Lower Cretaceous, Spain): A phenetic correlation approach. *Palaeoworld* **2024**. [CrossRef]
57. Sanz, J.L.; Buscalioni, A.D.; Casanovas, M.L.; Santafé, J.V. Dinosaurios del Cretácico Inferior de Galve (Teruel, España). *Estud. Geol.* **1987**, *43*, 45–64.
58. Sánchez-Hernández, B.; Benton, M.J.; Naish, D. Dinosaurs and other fossil vertebrates from the Late Jurassic and Early Cretaceous of the Galve area, NE Spain. *Palaeogeogr. Palaeoclimatol. Palaeoecol.* **2007**, *249*, 180–215.
59. Ruiz-Omeñaca, J.I.; Canudo, J.I.; Cruzado-Caballero, P.; Infante, P.; Moreno-Azanza, M. Baryonychine teeth (Theropoda: Spinosauridae) from the Lower Cretaceous of La Cantalera (Josa, NE Spain). *Kaupia* **2005**, *14*, 59–63.
60. Sánchez-Hernández, B.; Benton, M.J. Filling the ceratosaur gap: A new ceratosaurian theropod from the Early Cretaceous of Spain. *Acta Palaeontol. Pol.* **2012**, *59*, 581–600.
61. Rauhut, O.W.M.; Canudo, J.I.; Castanera, D. A reappraisal of the Early Cretaceous theropod dinosaur *Camarillasaurus* from Spain. In *Program and Abstracts XVII Conference of the EAVP*; European Association of Vertebrate Paleontologists (EAVP), Ed.; European Association of Vertebrate Paleontologists: Brussels, Belgium, 2019; p. 96.

62. Malafaia, E.; Gasulla, J.M.; Escaso, F.; Narvaéz, I.; Ortega, F. An update of the spinosaurid (Dinosauria: Theropoda) fossil record from the Lower Cretaceous of the Iberian Peninsula: Distribution, diversity, and evolutionary history. *J. Iber. Geol.* **2020**, *46*, 431–444.
63. Samathi, A.; Sander, P.M.; Chanthasit, P. A spinosaurid from Thailand (Sao Khua Formation, Early Cretaceous) and a reassessment of *Camarillasaurus cirugedae* from the Early Cretaceous of Spain. *Hist. Biol.* **2021**, *33*, 3480–3494. [CrossRef]
64. Estes, R.; Sanchiz, B. Early cretaceous lower vertebrates from Galve (Teruel), Spain. *J. Vertebr. Paleontol.* **1982**, *2*, 21–39.
65. Ruiz-Omeñaca, J.I.; Canudo, J.I.; Aurell, M.; Bádenas, B.; Barco, J.L.; Cuenca-Bescós, G.; Ipas, J. Estado de las investigaciones sobre los vertebrados del Jurásico Superior y Cretácico Inferior de Galve (Teruel). *Estud. Geol.* **2004**, *60*, 179–202.
66. Pérez-García, A.; Murelaga, X. *Larachelus morla*, gen. et sp. nov. a new member of the little-known European Early Cretaceous record of stem cryptodiran turtles. *J. Vertebr. Paleontol.* **2012**, *32*, 1293–1302.
67. Pérez-García, A.; Scheyer, T.M.; Murelaga, X. The turtles from the uppermost Jurassic and Early Cretaceous of Galve (Iberian Range, Spain): Anatomical, systematic, biostratigraphic and palaeobiogeographical implications. *Cretac. Res.* **2013**, *44*, 64–82.
68. Buscalioni, A.D.; Sanz, J.L. Cocodrilos del Cretácico inferior de Galve (Teruel, España). *Estud. Geol.* **1987**, *43*, 23–43.
69. Arribas, I.; Buscalioni, A.D.; Royo-Torres, R.; Espílez, E.; Mampel, L.; Alcalá, L. A new goniopholidid crocodyliform, Hulkepholis rori sp. nov. from the Camarillas Formation (early Barremian) in Galve, Spain. *PeerJ* **2019**, *7*, e7911.
70. Canudo, J.I.; Cuenca-Bescos, G. Two new mammalian teeth (Multituberculata and Peramura) from the Lower Cretaceous (Barremian) of Spain. *Cretac. Res.* **1996**, *17*, 215–228.
71. Badiola, A.; Canudo, J.I.; Cuenca-Bescós, G. A systematic reassessment of Early Cretaceous multituberculates from Galve (Teruel, Spain). *Cretac. Res.* **2011**, *32*, 45–57.
72. Delvene, G.; Munt, M.C.; Royo-Torres, R.; Cobos, A. *Monginaia*, a new genus of endemic bivalve from the lower Barremian of Teruel, eastern Spain, and the distribution of unionid bivalves in Spanish Cretaceous. *Cretac. Res.* **2022**, *138*, 105268.
73. Skeletal Drawing. Available online: https://www.skeletaldrawing.com/ (accessed on 11 June 2024).
74. Hammer, Ø.; Harper, D.; Ryan, P. PAST: Paquete de programas de estadística paleontológica para enseñanza y análisis de datos. *Palaeontol. Electron.* **2001**, *4*, 9.
75. Marsh, O.C. Principal characters of American Jurassic dinosaurs, part V. *Am. J. Sci.* **1881**, *3*, 417–423.
76. Madzia, D.; Arbour, V.M.; Boyd, C.A.; Farke, A.A.; Cruzado-Caballero, P.; Evans, D.C. The phylogenetic nomenclature of ornithischian dinosaurs. *PeerJ* **2021**, *9*, e12362.
77. Dollo, L. Iguanodontidae et Camptonotidae. *Comptes Rendus De L'académie Des Sci.* **1888**, *106*, 775–777.
78. Sereno, P.C. Phylogeny of the bird-hipped dinosaurs (Order Ornithischia). *Natl. Geogr. Res.* **1986**, *2*, 234–256.
79. Sánchez-Fenollosa, S.; Verdú, F.J.; Cobos, A. The largest ornithopod (Dinosauria: Ornithischia) from the Upper Jurassic of Europe sheds light on the evolutionary history of basal ankylopollexians. *Zool. J. Linn. Soc.* **2023**, *199*, 1013–1033.
80. Sereno, P.C. The origin and evolution of dinosaurs. *Annu. Rev. Earth Planet. Sci.* **1997**, *25*, 435–489.
81. Sereno, P.C. A rationale for phylogenetic definitions, with application to the higher-level taxonomy of Dinosauria. *Neues Jahrb. Für Geol. Und Paläontologie Abh.* **1998**, *210*, 41–83. [CrossRef]
82. Mantell, G.A. Notice on the *Iguanodon*, a newly discovered fossil reptile, from the sandstone of Tilgate Forest, in Sussex. *Philos. Trans. R. Soc.* **1825**, *115*, 179–186.
83. Griffin, C.T.; Stocker, M.R.; Colleary, C.; Stefanic, C.M.; Lessner, E.J.; Riegler, M.; Formoso, K.; Koeller, K.; Nesbitt, S.J. Assessing ontogenetic maturity in extinct saurian reptiles. *Biol. Rev.* **2020**, *96*, 470–525.
84. Norman, D.B. Iguanodonts from the Wealden of England: Do they to contribute to the discussion concerning hadrosaur origins? In *Hadrosaurs*; Eberth, D.A., Evans, D.C., Eds.; Indiana University Press: Bloomington, IN, USA, 2014; pp. 10–43.
85. Brochu, C.A. Closure of neurocentral sutures during crocodilian ontogeny: Implications for maturity assessment in fossil archosaurs. *J. Vertebr. Paleontol.* **1996**, *16*, 49–62. [CrossRef]
86. Ikejeri, T. Histology-based morphology of the neurocentral synchondrosis in *Alligator mississippiensis* (Archosauria, Crocodylia). *Anat. Rec. Adv. Integr. Anat. Evol. Biol.* **2012**, *295*, 18–31.
87. Galton, P.M. *Dryosaurus*, a hypsilophodontid dinosaur from the Upper Jurassic of North America and Africa. Postcranial skeleton. *Paläontologische Z.* **1981**, *55*, 272–312.
88. Hübner, T. The postcranial ontogeny of *Dysalotosaurus lettowvorbecki* (Ornithischia: Iguanodontia) and implications for the evolution of ornithopod dinosaurs. *Palaeontogr. Abt. A Palaeozoology—Stratigr.* **2018**, *310*, 43–120. [CrossRef]
89. Verdú, F.J. Sistemática, Filogenia y Paleobiología de *Iguanodon galvensis* (Ornithopoda, Dinosauria) del Barremiense Inferior (Cretácico Inferior) de Teruel (España). Ph.D. Thesis, Universidad de Valencia, Valencia, Spain, 2017.
90. Romer, A.S. *Osteology of the Reptiles*; University of Chicago Press: Chicago, IL, USA, 1956; p. 772.
91. Horner, H.R.; Weishampel, D.B.; Forster, C.A. Hadrosauridae. In *The Dinosauria*, 2nd ed.; Weishampel, D.B., Donson, P., Osmólska, H., Eds.; University of California Press: Berkeley, CA, USA, 2004; pp. 438–463.
92. Moro, D.; Kerber, L.; Müller, R.T.; Pretto, F.A. Sacral co-ossification in dinosaurs: The oldest record of fused sacral vertebrae in Dinosauria and the diversity of sacral co-ossification patterns in the group. *J. Anatom.* **2021**, *238*, 828–844.
93. Taquet, P. *Géologie et Paléontologie du Gisement de Gadoufaoua (Aptien du Niger)*; Éditions du Centre National de la Recherche Scientifique: Paris, France, 1976; p. 191.
94. Cuthbertson, R.S.; Holmes, R.B. The first complete description of the holotype of *Brachylophosaurus canadensis* Sternberg, 1953 (Dinosauria: Hadrosauridae) with comments on intraspecific variation. *Zool. J. Linn. Soc.* **2010**, *159*, 373–397.

95. Xing, H.; Mallon, J.C.; Currie, M.L. Supplementary cranial description of the types of *Edmontosaurus regalis* (Ornithischia: Hadrosauridae), with comments on the phylogenetics and biogeography of Hadrosaurinae. *PLoS ONE* **2017**, *12*, e0175253.
96. Godefroit, P.; Bolotsky, Y.L.; Bolotsky, I.Y. Osteology and relationships of *Olorotitan arharensis*, a hollow-crested hadrosaurid dinosaur from the latest Cretaceous of Far Eastern Russia. *Acta Palaeontol. Pol.* **2012**, *57*, 527–560.
97. Knoll, F. A large iguanodont from the upper Barremian of the Paris Basin. *Geobios* **2009**, *42*, 755–764. [CrossRef]
98. Norman, D.B. Basal Iguanodontia. In *The Dinosauria*; Weishampel, D.B., Dodson, P., Osmólska, H., Eds.; University California Press: Berkeley, CA, USA, 2004; pp. 413–437.
99. Gilmore, C.W. *Osteology of the Jurassic Reptile Camptosaurus: With a Revision of the Species of the Genus, and Description of two New Species*; Washington Smithsonian Institution Press: Washington, DC, USA, 1909; Volume 36, pp. 197–332. [CrossRef]
100. McDonald, A.T.; Kirkland, J.I.; DeBlieux, D.D.; Madsen, S.K.; Cavin, J.; Milner, A.R.; Panzarin, L. New basal iguanodonts from the Cedar Mountain Formation of Utah and the evolution of thumb-spiked dinosaurs. *PLoS ONE* **2010**, *5*, e14075.
101. McDonald, A.T.; Maidment, S.C.; Barrett, P.M.; You, H.L.; Dodson, P. Osteology of the basal hadrosauroid *Equijubus normani* (Dinosauria, Ornithopoda) from the Early Cretaceous of China. In *Hadrosaurs*; Eberth, D.A., Evans, D.C., Eds.; Indiana University Press: Bloomington, IN, USA, 2014; pp. 44–72.
102. Bertozzo, F.; Dalla Vecchia, F.M.; Fabbri, M. The Venice specimen of *Ouranosaurus nigeriensis* (Dinosauria, Ornithopoda). *PeerJ* **2017**, *5*, e3403. [PubMed]
103. Medrano-Aguado, E.; Parrilla-Bel, J.; Gasca, J.M.; Alonso, A.; Canudo, J.I. Ornithopod diversity in the Lower Cretaceous of Spain: New styracosternan remains from the Barremian of the Maestrazgo Basin (Teruel province, Spain). *Cretac. Res.* **2023**, *144*, 105458.